Author/s:
Wu, H;Praveen, P;Handley, TNG;Chandrashekar, C;Cummins, SF;Bathgate, RAD;Hossain, MA

Title:
Total Chemical Synthesis of Aggregation-Prone Disulfide-Rich Starfish Peptides

Date:
2024-06-12

Citation:
Wu, H., Praveen, P., Handley, T. N. G., Chandrashekar, C., Cummins, S. F., Bathgate, R. A. D. & Hossain, M. A. (2024). Total Chemical Synthesis of Aggregation-Prone Disulfide-Rich Starfish Peptides. Chemistry A European Journal, 30 (33), https://doi.org/10.1002/chem.202400933.

Persistent Link:
https://hdl.handle.net/11343/351071

Chemistry–A European Journal
Research Article
doi.org/10.1002/chem.202400933
Chemistry Europe
European Chemical Societies Publishing
www.chemeurj.org

Total Chemical Synthesis of Aggregation-Prone Disulfide-Rich Starfish Peptides

Hongkang Wu,[a] Praveen Praveen,[a] Thomas N. G. Handley,[a] Chaitra Chandrashekar,[a] Scott F. Cummins,[b, c] Ross A. D. Bathgate,[a, d] and Mohammed Akhter Hossain*[a, e]

A relaxin-like gonad-stimulating peptide (RGP), Aso-RGP, featuring six cysteine residues, was identified in the Crown-of-Thorns Starfish (COTS, Acanthaster cf. *solaris*) and initially produced through recombinant yeast expression. This method yielded a single-chain peptide with an uncleaved C-peptide (His Tag) and suboptimal purity. Our objective was to chemically synthesize Aso-RGP in its mature form, comprising two chains (A and B) and three disulfide bridges, omitting the C-peptide. Furthermore, we aimed to synthesize a newly identified relaxin-like peptide, Aso-RLP2, from COTS, which had not been previously synthesized. This paper reports the first total chemical synthesis of Aso-RGP and Aso-RLP2. Aso-RGP synthesis proceeded without major issues, whereas the A-chain of Aso-RLP2, in its reduced and unfolded state with two free thiols, presented considerable challenges. These were initially marked by "messy" RP-HPLC profiles, typically indicative of synthesis failure. Surprisingly, oxidizing the A-chain significantly improved the RP-HPLC profile, revealing the main issue was not synthesis failure but the peptide's aggregation tendency, which initially obscured analysis. This discovery highlights the critical need to account for aggregation in peptide synthesis and analysis. Ultimately, our efforts led to the successful synthesis of both peptides with purities exceeding 95 %.

Introduction

Insulin and relaxin-like peptides (RLPs) are a diverse family of hormones with pivotal roles in various physiological processes in mammals.[1] Ten key members of this family have been identified in humans; insulin,[2] insulin-like growth factor I[3] and II,[4] and 7 relaxin sub-family peptides that include relaxin-1 (H1 relaxin),[5] relaxin-2 (H2 relaxin),[6] relaxin-3 (H3 relaxin),[7] insulin-like peptide 3 (INSL3),[8] INSL4,[9] INSL5,[10] and INSL6.[7] A shared structural motif that defines insulin and RLPs consists of two chains (A- and B-chain) joined by two inter-chain disulfide bonds, and a third disulfide bond within the A-chain; together the three disulfides provide structural stability to RLPs. The conservation of the disulfide motif, despite high levels of sequence variation elsewhere in RLPs, highlights the evolutionary significance of maintaining a specific three-dimensional architecture.[11]

The initial discovery of RLPs primarily focused on mammalian systems, with the relaxin peptide (relaxin-2 in humans, relaxin-1 in non-primates) being identified as a key player in reproductive processes.[12] As research methodologies have advanced, RLPs have been identified in a broad range of organisms, including invertebrates and non-mammalian vertebrates.[11,13] In 2009, a relaxin-like peptide was identified and biochemically characterized as a 'gonad-stimulating substance' in the starfish *Asterina pectinifera*.[14] It is named a relaxin-like gonad-stimulating peptide (RGP)[15] and is secreted by radial nerves to induce follicular cells to produce 1-methyladenine, the echinoderm counterpart of vertebrate progestin, thereby promoting oocyte maturation. RGPs have subsequently been found in diverse starfish species.[16]

The Crown-of-Thorns Starfish (COTS; *Acanthaster* cf. *solaris*) is an echinoderm of considerable interest due to its devastating impact on the world's coral reef ecosystems when at high density.[17] COTS RGP (Aso-RGP; Figure 1A) has been previously generated recombinantly through a yeast expression system to demonstrate its efficacy in inducing oocyte maturation and ovulation *in vitro*, showcasing its potential as a pivotal player in the reproductive processes of mature female COTS.[18] In more recent investigations employing genome and transcriptome analyses focused on RLPs in marine organisms, a second relaxin-like peptide, named RLP2 has been successfully identified in multiple starfish species including COTS, namely Aso-RLP2 (Figure 1B).[16d] The identification of this novel Aso-RLP2 prompts an intriguing inquiry into its potential *in vitro* activity in comparison to Aso-RGP. As such, exploring the functional

[a] H. Wu, Dr. P. Praveen, Dr. T. N. G. Handley, Dr. C. Chandrashekar, Prof. R. A. D. Bathgate, Prof. M. A. Hossain
The Florey, The University of Melbourne, Victoria, Australia
[b] Prof. S. F. Cummins
Centre for Bioinnovation, University of the Sunshine Coast, Queensland, Australia
[c] Prof. S. F. Cummins
School of Science, Technology and Engineering, University of the Sunshine Coast, Queensland, Australia
[d] Prof. R. A. D. Bathgate
Department of Biochemistry and Pharmacology, The University of Melbourne, Victoria, Australia
[e] Prof. M. A. Hossain
School of Chemistry, The University of Melbourne, Victoria, Australia
E-mail: akhter.hossain@unimelb.edu.au

Supporting information for this article is available on the WWW under https://doi.org/10.1002/chem.202400933

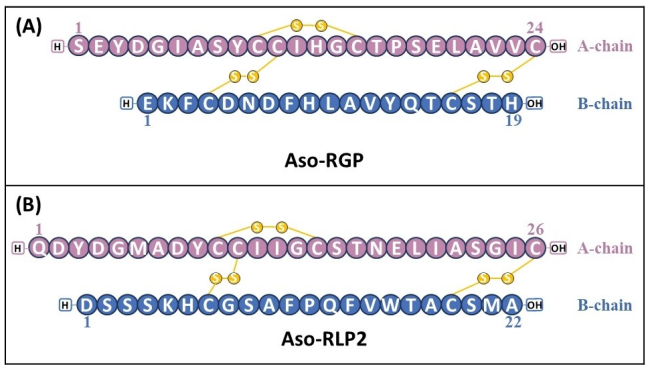

Figure 1. Schematic diagram of the chemical sequence of (A) Aso-RGP and (B) Aso-RLP2.

dynamics and comparative activities of Aso-RGP and Aso-RLP2 may unveil essential insights into the diverse role played by these peptides in the reproductive physiology of COTS. To undertake such investigations, the imperative first step is the precise generation of these peptides.

The successful synthesis of these peptides will not only serve as a methodological advancement but will also pave the way for in-depth molecular analyses, shedding light on the intricacies of reproductive neuroendocrine physiology in COTS. However, the conserved structural scaffold (two-chain and three-disulfide bonds) of RLPs, while fundamental for their biological activity, represents a significant challenge in the production both recombinantly[19] and chemically.[20] Recombinant synthesis often faces hurdles in achieving proper post-translational modifications and correct disulfide linkages, impacting the peptides' functionality. Aso-RLP2 peptide has never been synthesized, either chemically or recombinantly. Although Aso-RGP has been recombinantly synthesized previously, the resulting construct was not a mature hormone, featuring a B-chain and A-chain with an extraneous histidine linker as connecting C-peptide.[18] Moreover, it is difficult to purify the recombinantly synthesized Aso-RGP to greater than 90% purity, which may compromise *in vitro* and *in vivo* analysis.[18] To address these limitations and contribute to a more nuanced molecular analysis, this research is dedicated to the first chemical synthesis of both Aso-RGP and Aso-RLP2.

Regioselective chemical synthesis of RLPs requires a separate synthesis of the A- and B-chain and then various chemical reactions to combine the two chains in correctly folded form to yield the final products. The synthesis of the A- and B-chains may individually pose considerable challenges often primarily due to their inherent hydrophobicity and aggregating tendencies. For example, the A-chain of structurally related peptides like human insulin and INSL5 was found to be extremely hydrophobic and aggregating in nature hindering both their chemical assembly and purification.[21] As we embarked on the chemical synthesis of Aso-RGP and Aso-RLP2, addressing the aggregating tendencies of the A-chain became a central focus, requiring meticulous optimization to achieve successful peptide assembly while preserving its native conformation.

In this study, we report the first chemical synthesis of two peptides, Aso-RGP and Aso-RLP2 (the peptides that have complex insulin-like chemical structure - two chains, three disulfide bridges) using Fmoc-solid-phase peptide synthesis (Fmoc-SPPS) followed by stepwise regioselective disulfide bond formation strategy.[21b,22] The chemical synthesis of Aso-RGP was found to be relatively straightforward resulting in a final product with high purity (>95%). However, the synthesis of the Aso-RLP2 posed notable challenges mainly with the assembly of the A-chain, involving strategic adaptations to overcome challenges associated with the A-chain's aggregating nature. Notably, three distinct attempts were made, employing various coupling agents and refined strategies, ultimately leading to the successful chemical synthesis of the A-chain, which was then used for successful conjugation with its B-chain to yield the final product Aso-RLP2 with over 98% purity.

Results and Discussion

In the pursuit of synthesizing RLPs, our laboratory has traditionally employed Fmoc-SPPS in conjunction with regioselective disulfide formation methods, achieving successful chemical synthesis of numerous peptides.[20a,23] In this study, we applied similar methodologies for the synthesis of Aso-RGP (Scheme 1) and Aso-RLP2 (Scheme 2). The synthesis of Aso-RGP proceeded smoothly, yielding a high-purity final product with over 95% purity. Conversely, the synthesis of Aso-RLP2 posed a more intricate challenge, requiring iterative attempts and methodological adjustments to achieve successful synthesis.

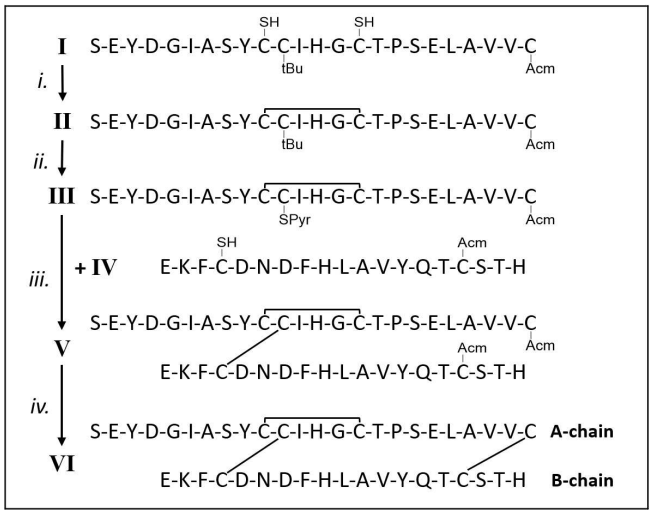

Scheme 1. Regioselective disulfide bond formation of Aso-RGP (compound **VI**). (*i.*) The A-chain **I** is oxidized to form the intramolecular disulfide bond, producing **II**; (*ii.*) Conversion of Cys(tBu)^{A11} to Cys(SPyr)^{A11}, producing **III**; (*iii.*) **III** combined with the B-chain **IV** to form the first interchain bond via thiolysis, producing **V**; (*iv.*) Iodine oxidation forms the last disulfide bond, producing the final product **VI**. Detailed conditions are outlined in the Experimental Section.

Scheme 2. Regioselective disulfide bond formation of Aso-RLP2 (compound **6**). (*i.*) The A-chain **1** is oxidized to form the intramolecular disulfide bond, producing **2**; (*ii.*) Conversion of Cys(tBu)^{A11} to Cys(SPyr)^{A11}, producing **3**; (*iii.*) **3** combined with the B-chain **4** to form the first interchain bond via thiolysis, producing **5**; (*iv.*) Iodine oxidation forms the last disulfide bond, producing the final product **6**. Z: Pyroglutamic acid. Detailed conditions are outlined in the Experimental Section.

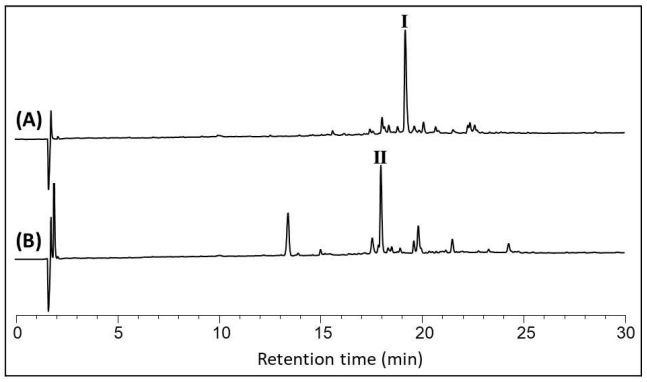

Figure 2. RP-HPLC monitoring of the oxidation reaction (Scheme 1, *i.*). (A) RP-HPLC analysis of the crude A-chain of Aso-RGP, compound **I**; (B) RP-HPLC analysis of an aliquot of A-chain oxidation reaction mixture after 30 minutes reaction time, showing the formation of **II** (Aso-RGP A-chain with intra-disulfide formed). RP-HPLC analysis was carried out using the elution gradient: 15–45 % Buffer B in 30 minutes.

Comparative Complexity of the A-Chain Synthesis

Initially, for the A-chain of both Aso-RGP and Aso-RLP2 (compound **I** and **1** respectively, Schemes 1, 2), we used Fmoc-Cys(Acm) preloaded TentaGel® S PHB resin and employed DIC/Oxyma as the coupling agent. All the residues within the sequence were coupled via the microwave-assisted automatic synthesizer. Coupling was performed using 6 equivalents of each amino acid activated by Oxyma (6 equivalents) and DIC (6 equivalents) in DMF at 75 °C for 10 minutes (detailed synthesis conditions in Experimental Section).

Following cleavage, the crude A-chain of Aso-RGP (**I**, Scheme 1) exhibited a discernible major peak in reversed-phase high-performance liquid chromatography (RP-HPLC) analysis (Figure 2A), affirming the successful synthesis of a high-quality product. Subsequently, the crude A-chain **I** was directly employed in the oxidation reaction to form the intra-A-chain disulfide bond (scheme 1, *i.*), resulting in a successful reaction with an evident leftward shift in the RP-HPLC chromatography (Figure 2B). This allowed for a smooth transition of the oxidized A-chain to the subsequent chemical reaction (Scheme 1, *ii.*) and successful conjugation with its corresponding B-chain (Scheme 1, *iii.* and *iv.*), culminating in the generation of the final product (**VI**, Scheme 1) without complications (detailed reaction conditions are shown in the Experimental Section).

In contrast, the chemical synthesis of the A-chain of Aso-RLP2 (**1**, Scheme 2) proved to be more challenging, with the crude A-chain displaying a complex and messy RP-HPLC analytical profile (Figure 3A (a)). Therefore, multiple attempts were made, incorporating diverse coupling conditions in an effort to enhance the synthesis quality.

In the second attempt, we switched to HATU/DIEA as the coupling agents. This time, all the residues were coupled manually at room temperature with a 6-fold molar excess of Fmoc-protected amino acids that were activated by HATU (5.8 equivalents) and DIEA (10 equivalents) for 1 hour. The analytical RP-HPLC profile of the cleaved peptide using these conditions was also observed to be still messy (Figure 3A (b)), further emphasizing the challenges encountered in achieving a clean and well-defined synthesis.

After two apparent failed attempts, we hypothesized that Aso-RLP2 contains a difficult peptide sequence in the A-chain that might aggregate during chain elongation and be prone to aspartimide formation due to the presence of Asp and Gly at positions A4 and A5 respectively. Thus, we explored a third strategy where we used a pseudoproline dipeptide 'Fmoc-Ser(tBu)-Thr($\Psi^{Me,Me}$pro)-OH'[24] at Ser-16 and Thr-17 to overcome aggregation during the peptide chain assembly, and a dipeptide 'Fmoc-Asp(OtBu)-(Dmb)Gly-OH' at Asp-4 and Gly-5 to overcome potential aspartimide formation.[25] These are established methods scientists use to synthesize difficult peptides. Indeed, we previously utilized this strategy to accomplish the successful synthesis of numerous difficult RLPs.[26] All the other residues were coupled manually using standard Fmoc-protected amino acids and HATU/DIEA as coupling agents. Despite these refinements, to our surprise, the analytical RP-HPLC profile of cleaved peptide using the third attempt still exhibited significant disordered peaks (Figure 3A (c)).

It was quite interesting to notice that the MALDI-8020 matrix-assisted laser desorption ionization time-of-flight mass spectrometer (MALDI-TOF MS) characterization of the crude peptides synthesized using the three attempts described above (Figure 3A (a–c)), displayed the desired mass as a major peak (Figure 3B). Thus, we hypothesized that we synthesized the peptide successfully, but it aggregates in solution during RP-HPLC analysis and thus we did not see a well-defined major peak. We have tried different columns (C4 vs C18) and different RP-HPLC solvents (acetonitrile vs isopropanol/ acetonitrile) and

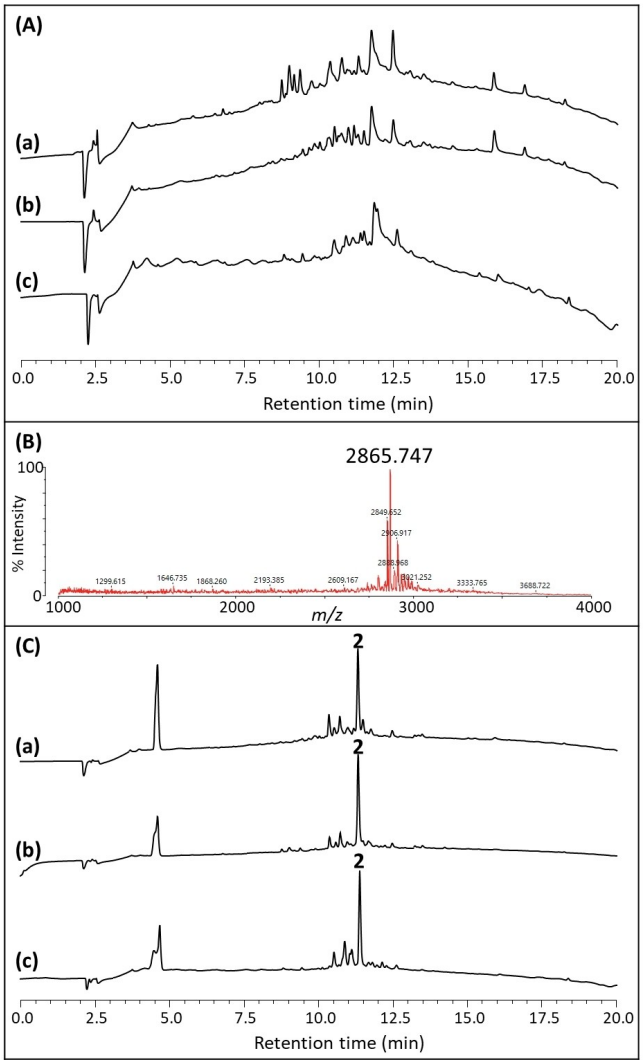

Figure 3. The crude A-chain of Aso-RLP2 (compound **1**) post-cleavage showed a disordered RP-HPLC profile, indicating a suboptimal quality of synthesis, while oxidation reaction directly on aggregated compound **1** successfully yielded the oxidized A-chain **2** (A-chain with intra-disulfide formed). (A) RP-HPLC analysis of crude compound **1** synthesized using (a) DIC/Oxyma as the coupling agent; (b) HATU/DIEA as the coupling agent; (c) HATU/DIEA as the coupling agent, together with the incorporation of pseudoproline and Asp-Gly dipeptide. (B) MALDI-TOF MS of crude compound **1**. (C) RP-HPLC analysis of an aliquot of A-chain oxidation reaction mixture after 30 minutes using the crude compound **1** synthesized using (a) DIC/Oxyma as the coupling agent; (b) HATU/DIEA as the coupling agent; (c) HATU/DIEA as the coupling agent, together with the incorporation of pseudoproline and Asp-Gly dipeptide. RP-HPLC analysis was carried out using the elution gradient: 0–100 % Buffer B in 20 minutes.

they did not improve the analytical RP-HPLC profiles. Furthermore, we attempted to optimize the analytical and purification profiles by increasing the temperature to 40 °C, hypothesizing that higher temperatures might disrupt peptide aggregates. Despite this adjustment, the RP-HPLC profiles remained complex and disordered, indicating that temperature alone was insufficient to mitigate aggregation. Subsequently, we employed a 6 M guanidine hydrochloride buffer (pH 5–6), aiming to enhance solubility and achieve clearer RP-HPLC analysis. Guanidine hydrochloride is well-recognized for its potent chaotropic properties, which can disrupt the hydrogen bonding network and reduce hydrophobic interactions among peptide molecules, thereby mitigating aggregation tendencies. However, this attempt also did not help to reveal a distinct major peak. These approaches and results underscored the persistent challenge of peptide aggregation, demonstrating that neither temperature increase nor solubilization with GnHCl buffer could fully overcome the inherent aggregation tendencies in chromatographic processes. Above all, the lack of a clear major peak rendered the purification of this product impractical, hindering advancement to the subsequent reaction stages as delineated in Scheme 2. Thus, we made a strategic decision to proceed to the next oxidation reaction (Scheme 2 *i.*) directly on the crude A-chain without seeing a clean RP-HPLC analysis profile. Surprisingly, the oxidation reactions of crude A-chain from three distinct attempts all resulted in the desired product (compound **2**, Scheme 2) with a major, well-defined peak (Figure 3C (a–c)). This unexpected clarity in the analytical RP-HPLC profiles post-oxidation implies that the initially disordered profiles of the crude peptides have arisen from successful synthesis yet are hindered by the aggregating nature of the peptides during analysis. The oxidation process, forming the intra-disulfide bond, seemingly mitigated the aggregation, resulting in the production of a clear major RP-HPLC peak.

This phenomenon of improved behavior following the oxidation of the A-chain closely aligns with observations from the synthesis of human Se-insulin,[27] an analogue of insulin that shares a similar structural framework with RLPs, characterized by a two-chain, three-disulfide-bonded architecture. In the case of human Se-insulin, the innovative strategy of incorporating a diselenide bond specifically between residues A6 and A11 within its A chain has led to the production of a seleno-A chain. This modification notably enhanced the solubility of the chain and significantly reduced its tendency to aggregate.[27] Such findings are instrumental in dispelling the myth of 'failed synthesis' by demonstrating how chemical modifications can profoundly affect peptide solubility and behavior.

This unanticipated success underscores the nuanced interplay between peptide aggregation and the effectiveness of subsequent chemical transformations, offering valuable insights for refining synthetic strategies in peptide chemistry. In light of these results, we can conclude that the incorporation of costly dipeptides, such as pseudoproline and Asp-Gly, is not essential for achieving an optimal synthesis of the A-chain for Aso-RLP2. Despite the initially challenging RP-HPLC analyses of the crude peptides, the successful outcome of the oxidation reactions indicated that the standard coupling conditions, employing all standard amino acids, could yield a comparable synthesis quality.

Conversion of Cys(tBu)^{A11} to Cys(SPyr)^{A11} of A-Chain of Aso-RLP2

Following the successful oxidation reaction, the next step involved the conversion of Cys(tBu)^{A11} to Cys(SPyr)^{A11} of the oxidized product **2** (Scheme 2 *ii.*). Compound **2** was purified

(Figure 4A) and used for the next step. This transformation necessitated the use of the strong acid TFMSA to selectively cleave off the tBu-protecting group at the residue Cys^{A11}. Simultaneously, the addition of dipyridyldisulfide (DPDS) in the cleavage cocktail facilitated the conversion of $Cys(SPyr)^{A11}$ during the cleavage process. The reaction yielded the anticipated product, denoted as compound **3** (Scheme 2). After cleavage, despite rigorous washes with ice-cold diethyl ether, traces of excess DPDS (Figure 4B) persisted in the crude peptide **3**, posing a challenge during the subsequent purification step.

The purification process of crude compound **3** yielded two distinct batches. One batch displayed a slightly lower purity with residual DPDS from the purification of the crude compound **3** (Figure 5A (a)), while the other batch exhibited no detectable DPDS, indicating a higher level of purity (Figure 5A (b)). Both batches were utilized in the subsequent combination reaction of the A- and B-chain (Scheme 2, *iii.*), aimed at forming the first inter-chain disulfide bond. This allowed the examination of the impact of varying purity levels on the success of the disulfide bond formation.

Chain Combination of Aso-RLP2

The crude B-chain of Aso-RLP2 (compound **4**, Scheme 2) was purified and obtained with high purity (Figure 5B). Here, using the purified compound **4** and two different batches of A-chain (Figure 5A (a–b)), we conducted combination reactions to form the first inter-chain disulfide bond (Scheme 2, *iii.*).

The first combination reaction involved an A-chain with unintentional suboptimal purity, resulting from the challenging separation of residual DPDS during the prior purification of compound **3**. In this reaction, a notable suboptimality in cleanliness was observed and there was the formation of many byproducts during the combination reaction (Figure 5C (a)).

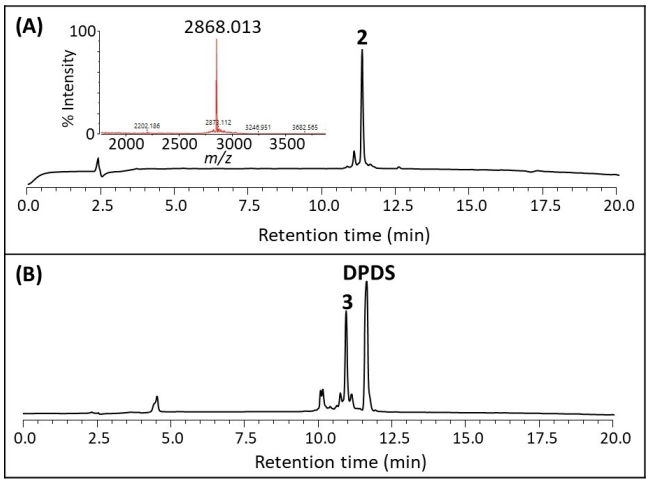

Figure 4. Conversion of $Cys(tBu)^{A11}$ of the compound **2** to $Cys(SPyr)^{A11}$, producing compound **3** (oxidized A-chain with SPyr attached to Cys^{A11}), (Scheme 2 *ii.*). (A) RP-HPLC analysis and MALDI-TOF MS of purified **2**. (B) RP-HPLC profile of the crude **3** post-conversion cleavage, showing traces of excess DPDS remained in the crude material. RP-HPLC analysis was carried out using the elution gradient: 0–100 % Buffer B in 20 minutes.

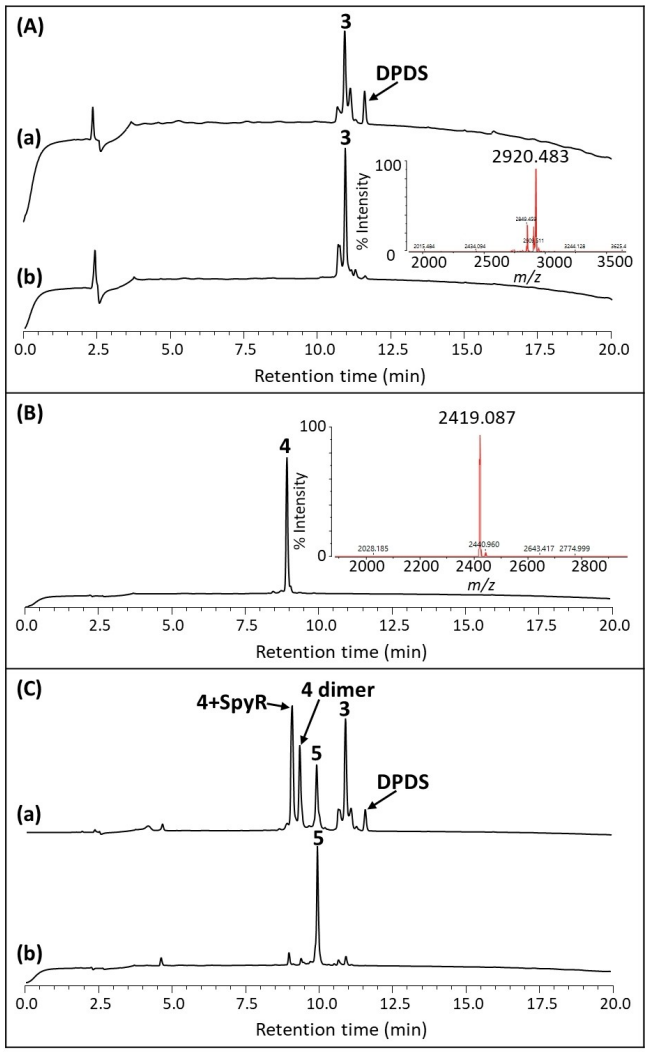

Figure 5. Combination reaction of compound **3** (A-chain) and compound **4** (B-chain) (Scheme 2 *iii.*). (A) RP-HPLC analysis of two batches of the purified compound **3**: (a) with residual DPDS (b) with no residual DPDS and with a higher level of purity; (B) RP-HPLC analysis and MALDI-TOF MS of purified compound **4**; (C) Comparative RP-HPLC profiles of chain combination reactions using A-chains with varied purity: (a) RP-HPLC profile corresponds to the combination reaction involving a purified compound **3** with unintentional suboptimal purity, marked by the presence of residual DPDS due to difficult separation during previous purification of compound **3**; (b) RP-HPLC profile represents the combination reaction with a purified compound **3**, free from residual DPDS. RP-HPLC analysis was carried out using the elution gradient: 0–100 % Buffer B in 20 minutes.

This is evident that the presence of DPDS significantly impacted the reaction, emphasizing its negative influence on the overall outcome of RLP combination reactions.

Conversely, the reaction employed a meticulously purified A-chain, ensuring the complete removal of DPDS from the previous purification step, proceeded with a discernible increase in efficiency, and the desired product was obtained with high yield and great purity (Figure 5C (b)).

Iodine Oxidation to Produce the Final Product, Aso-RLP2

Following the successful combination reaction of the A- and B-chain of Aso-RLP2, purification was carried out to obtain purified compound **5** (Scheme 2, Figure 6A) for the final step which involved an iodine oxidation reaction aimed at forming the final disulfide bond (Scheme 2 *iv.*). Specifically, the Acm-groups at positions A26 and B19 were selectively removed, facilitating the formation of the last disulfide bond by treating with I_2. Notably, the oxidation reaction proceeded seamlessly, resulting in the formation of the desired product **6** (Scheme 2), where the efficiency of the reaction was evident from the RP-HPLC analysis of the crude material as a single sharp peak (Figure 6B). Subsequent to the successful reaction, the peptide was subjected to purification to obtain the final native folded product.

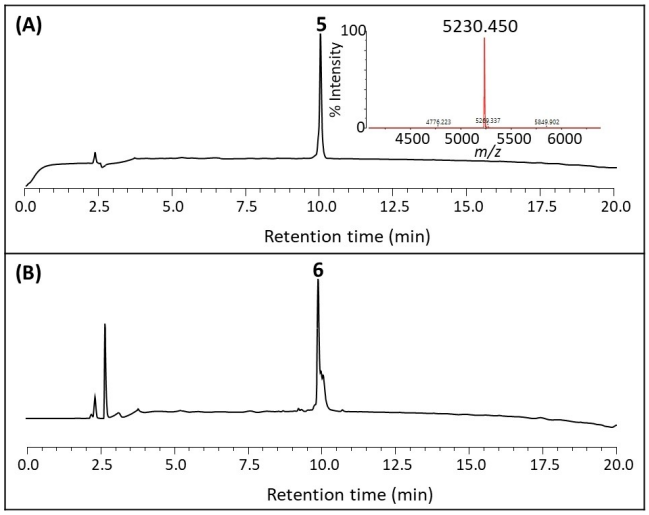

Figure 6. The iodine oxidation reaction of purified compound **5** to form the final product **6** (Aso-RLP2) (Scheme 2 *iv.*). (A) RP-HPLC profile and MALDI-TOF MS of purified **5**; (B) RP-HPLC analysis of crude **6**. RP-HPLC analysis was carried out using the elution gradient: 0–100% Buffer B in 20 minutes.

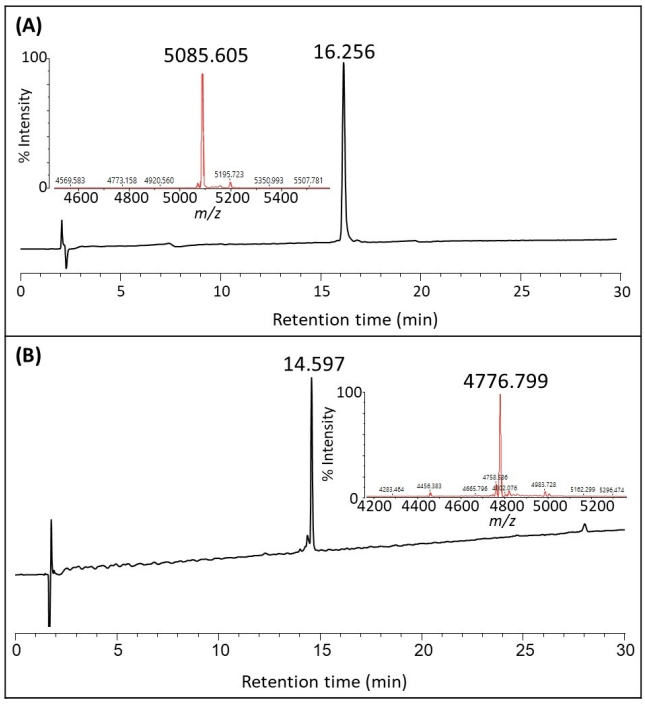

Figure 7. RP-HPLC analysis and MALDI-TOF MS of the purified final product. (A) Aso-RLP2, RP-HPLC was carried out using the elution gradient: 20–50% Buffer B in 30 minutes; and (B) Aso-RGP, RP-HPLC was carried out using the elution gradient: 15–45% Buffer B in 30 minutes.

Conformation of the Peptides

Leveraging the approach outlined in Schemes 1 and 2 for regioselective disulfide bond formation (detailed conditions outlined in the Experimental Section), we adeptly navigated the complex synthesis pathways to successfully produce the final peptides, Aso-RGP and Aso-RLP2, respectively. The overall yield for Aso-RLP2 was 8.7%, calculated from the purified B-chain, achieving a purity exceeding 98%, as confirmed by analytical RP-HPLC and MALDI-TOF MS analysis shown in Figure 7 A. Similarly, Aso-RGP was obtained with an overall yield of 6.2% calculated from its purified B-chain, surpassing 95% purity, as confirmed by analytical RP-HPLC and MALDI-TOF MS analysis shown in Figure 7B.

To assess and compare the conformational characteristics of Aso-RGP and Aso-RLP2, circular dichroism (CD) spectroscopy was employed as it is particularly well-suited for probing the overall secondary structure of peptides and proteins in solution. By juxtaposing the CD spectra of Aso-RLP2 and Aso-RGP, we could discern potential similarities or differences in their secondary structures, shedding light on the synthetic success, structural integrity, and potential activity of chemically synthesized Aso-RLP2 and Aso-RGP *in vitro* and *in vivo*.

In our CD spectroscopy studies, both peptides exhibited characteristic double minima at 208 and 222 nm (Figure 8), indicative of typical helical structures in a 10 mM phosphate buffer solution. Further quantitative analysis revealed significant differences in the α-helical content between the two peptides. Aso-RLP2 exhibited an α-helical content of 22.62%, determined from a mean residual ellipticity at 222 nm ($[\theta]_{222\,nm}$) in which 100% helicity was calculated as −35416.67 and the observed

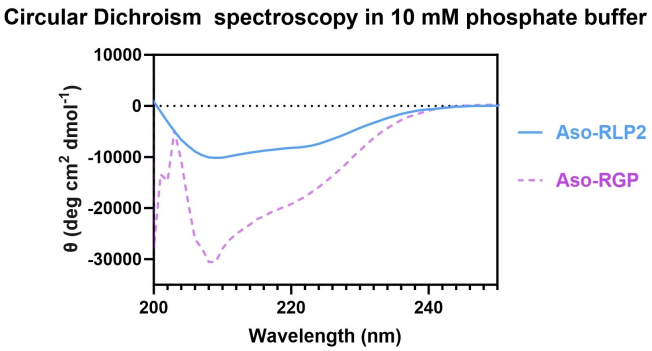

Figure 8. Circular dichroism spectrum of Aso-RLP2 (blue solid line) and Aso-RGP (purple dashed line). The CD was performed in 10 mM phosphate buffer at pH 7.4 at 25 °C.

$[\theta]_{222\,nm}$ was −8013.00. In contrast, the α-helical content of Aso-RGP was calculated to be 50.35%, determined from a calculated $[\theta]_{222\,nm}$ for 100% helicity of −35174.42 and an observed $[\theta]_{222\,nm}$ of −17709.17. This substantial helical content indicates a robust and stable helical structure in the Aso-RGP peptide, potentially influencing its biological activity and interaction with molecular targets. This discrepancy in helical content between the two peptides could be attributed to variations in their primary sequence, reflecting differences in their structural flexibility, solubility, or how each peptide interacts with its environment and binding partners.

Conclusions

In conclusion, this research represents a significant achievement in the successful chemical synthesis of Aso-RLP2 and Aso-RGP, marking the first instance of their chemical synthesis with high final product purity (>98% and >95%, respectively). To overcome challenges in the A-chain synthesis of Aso-RLP2, we strategically navigated through issues related to the aggregating nature of the peptide and observed that the incorporation of expensive dipeptides, such as pseudoproline and Asp-Gly, may not be imperative for achieving optimal synthesis quality. By streamlining the synthetic process to employ standard amino acids and standard coupling conditions, we not only enhanced cost-effectiveness, but also achieved a comparable synthesis quality. This successful synthesis not only provides a robust and adaptable methodology for Aso-RLP2 but also contributes valuable insights for advancing the broader field of peptide synthesis. We employed the regioselective disulfide formation strategy to control the correct folding of Aso-RLP2 and Aso-RGP in agreement with the native conformation. The synthesis of these peptides in good yield and purity, represents a crucial step toward unravelling their potential roles in COTS reproductive biology and underscores the importance of synthetic methodologies in advancing our understanding of marine peptide systems.

Experimental Section

Materials

9-Fluorenylmethoxycarbonyl (Fmoc) protected L-α-amino acids, 1-[Bis(dimethylamino)methylene]-1H-1,2,3-triazolo[4,5-b]pyridinium 3-oxide hexafluorophosphate (HATU), ethyl (hydroxyimino)cyanoacetate (Oxyma) and Fmoc-Histidine pre-loaded resin were purchased from Mimotopes (Australia). All amino acids were of L-configuration. Fmoc Cys(Acm) TentaGel® S PHB resin (0.21 mmol/g loading) was purchased from Rapp Polymere (Tübingen, Germany). TFMSA, diisopropylcarbodiimide (DIC), anisole, 3,6-dioxa-1,8-octanedithiol (DODT), N, N-diisopropylethylamine (DIEA), triisopropylsilane (TIPS), sinapinic acid (3,5-dimethyl-4-hydroxycinnamic acid), Fmoc-Ser(tBu)-Thr(Ψ^{Me}, ^{Me}pro)-OH, Fmoc-Asp(OtBu)-(Dmb)Gly-OH and piperidine were purchased from Sigma-Aldrich (Australia). 2,2′-Dipyridyldisulfide (DPDS) was purchased from Toronto Research Chemicals Inc. Trifluoroacetic acid (TFA), N, N-dimethylformamide (DMF), acetonitrile (ACN), Trizma® base, N-methyl morpholine (NMM), N-methylimidazole dichloromethane, diethyl ether and methanol were obtained from Merck Millipore and Sigma-Aldrich (Australia). MSNT, Amino-PEGA resin, and 4-(hydroxymethyl)phenoxyacetic acid (HMPA) were purchased from Novabiochem®. 6-Chloro-benzotriazole-1-yloxy-tris-pyrrolidinophosphonium hexafluorophosphate (PyClock) was purchased from ChemImpex (USA). All solvents were of analytical grade.

Fmoc-SPPS Peptide Synthesis

The detailed synthesis of the linear peptides of the individual chain via Fmoc-SPPS has been described in our previous publication.[26,28]

Fmoc-SPPS Synthesis of A-Chain of Aso-RLP2

The linear A-chain of Aso-RLP2 was assembled on Fmoc-Cys(Acm) preloaded TentaGel® S PHB resin (0.21 mmol/g loading, 0.05 mmol scale) via Fmoc-SPPS using three different coupling conditions, as outlined below. The sequence incorporated TFA-stable tert-butyl- (tBu−) and acetamidomethyl- (Acm−) protected Cys residues at the positions A11 and A26 positions, respectively (compound 1, Scheme 2). The Gln residue at the A1 position of the N-terminus of the A-chain was coupled as pyroglutamic acid (Z) as the free amino group of Gln is cyclized to form a lactam in the physiological environment.

DIC/Oxyma as the coupling agent: Automatic syntheses were performed to couple all the residues using a Biotage (Sweden) Initiator + Alstra microwave synthesizer. Coupling was performed using 6 equivalents of each amino acid activated by Oxyma (6 equivalents) and DIC (6 equivalents) in DMF at 75 °C for 10 minutes. Nα-Fmoc deprotection was achieved by treating with 20% v/v piperidine in DMF at room temperature for 2×5 minutes.

HATU/DIEA as the coupling agent: Manual syntheses were performed to couple all the residues at ambient temperature. All the residues were coupled with a 6-fold molar excess of Fmoc-protected amino acids that were activated by using a 5.8-fold excess of HATU in the presence of a 10-fold excess of DIEA. The coupling times were 1 hour for each coupling. Nα- Fmoc deprotection was carried out at ambient temperature by treating with 20% v/v piperidine in DMF for 2×5 minutes.

HATU/DIEA as the coupling agent together with the use of additional dipeptides: To reduce peptide aggregation during synthesis, the residues Ser^{A16} and Thr^{A17} of the A-chain were coupled as a single pseudoproline using Fmoc-Ser(tBu)-Thr(Ψ^{Me}, ^{Me}pro)-OH (2 equivalents) in the presence of PyClock (2 equivalents) and DIEA (1.0 M in DMF, 5 mL) overnight. Asp^{A4} and Gly^{A5} were coupled using Fmoc-Asp(OtBu)-(Dmb)Gly-OH (2 equivalents) in the presence of PyClock (2 equivalents) and DIEA (1.0 M in DMF, 5 mL) overnight to effectively prevent aspartimide formation at this position. Nα- Fmoc deprotection was carried out at ambient temperature by treating with 20% v/v piperidine in DMF for 2×5 minutes.

Fmoc-SPPS Synthesis of B-Chain of Aso-RLP2

The B-chain of Aso-RLP2 was synthesized on Amino-PEGA resin (0.37 mmol/g, 0.05 mmol scale) by Fmoc-SPPS. Manually, the resin was swollen in DMF overnight at ambient temperature. Coupling of HMPA linker (4 equivalents) was performed using HATU (3.8 equivalents) and NMM (8 equivalents) in DMF (3 mL) for 1 hour. This was followed by loading of the first amino acid (Fmoc-Ala-OH; 4 equivalents) in the presence of MSNT (4 equivalents) and N-methylimidazole (8 equivalents) in DCM (3 mL) and gently stirred at ambient temperature for 1 hour. The remaining sequence was

synthesized automatically using a Biotage (Sweden) Initiator+ Alstra microwave synthesizer. Coupling was performed using 6 equivalents of each amino acid activated by Oxyma (6 equivalents) and DIC (6 equivalents) in DMF at 75 °C for 10 minutes. Nα-Fmoc deprotection was achieved by treating with 20% v/v piperidine in DMF at room temperature for 2×5 minutes. The sequence contains an Acm-protected Cys at position B19 (compound 4, Scheme 2).

Fmoc-SPPS Synthesis of A- and B-Chain of Aso-RGP

The linear A- and B-chain of the Aso-RGP were synthesized automatically using a Biotage (Sweden) Initiator+ Alstra microwave synthesizer. Coupling was performed using 6 equivalents of each amino acid activated by Oxyma (6 equivalents) and DIC (6 equivalents) in DMF at 75 °C for 10 minutes. Nα-Fmoc deprotection was achieved by treating with 20% v/v piperidine in DMF at room temperature for 2×5 minutes. The A-chain (compound **I**, Scheme 1) was assembled on Fmoc-Cys(Acm) preloaded TentaGel® S PHB resin (0.21 mmol/g loading, 0.2 mmol scale), while the B-chain (compound **IV**, Scheme 1) was assembled on Fmoc-Histidine preloaded resin (0.523 mmol/g, 0.2 mmol scale). All side chain-protecting groups of amino acids were TFA-labile, except for tBu-protected Cys at position A11 and Acm-protected Cys at positions A24 and B16.

Standard Peptide Cleavage

After synthesis, the resin was washed 3× with DMF, and 3× with DCM and vacuum-dried for cleavage. The dried resin was treated with TFA:Anisol:H_2O:TIPS (93:3:2:2, 10 mL for every 0.1 mmol) cleavage cocktail for 1.5 hours at room temperature. Except for the tBu-protected Cys and the Acm-protected Cys, all the side chain protecting groups of amino acids are TFA-labile and thus were removed during the cleavage. After cleavage, the resin was filtered and the filtrate was concentrated under nitrogen flow, and then precipitated using ice-cold diethyl ether (10:1 diethyl ether:TFA volume after concentration). The pellet was washed by resuspending it in ice-cold diethyl ether 2 times and centrifuged for 2×10 minutes using Spintron Non-Refrigerated Mobile Centrifuge Model GT-175FR at speed 3500 Revolutions Per Minute (rpm). Finally, the washed pellet was air-dried overnight in a fume hood.

Peptide Purification, Analysis, and Characterization

Crude peptides were purified by RP-HPLC on a Phenomenex Gemini® C-18 column (150×21.2 mm, pore size 110 Å, particle size 5 μm) using a Shimadzu (Japan) Nexera preparative RP-HPLC that incorporates an SPD-M40 UV detector, at a flow rate of 10 mL/min. The aqueous buffer (buffer A) was 0.1% TFA in water, and the organic buffer (buffer B) was 0.1% TFA in ACN. The detection wavelength was set at 214 nm. The analysis of crude/purified compounds or the analysis of the reaction mixture was carried out on Phenomenex Gemini® C-18 column (250×4.6 mm, pore size 110 Å, particle size 5 μm) using a Shimadzu (Japan) Nexera analytical RP-HPLC that incorporates an SPD-M40 UV detector, at a constant flow rate of 1.5 mL/min, in the best appropriate gradient mode with the same buffer system as mentioned above. The molecular mass of peptides was determined using a Shimadzu MALDI-TOF MS using sinapinic acid as the matrix. The matrix was made up of 75% ACN containing 0.1% TFA.

Regioselective Disulfide Bond Formation of Aso-RLP2

A-Chain Oxidative Folding (Scheme 2 i.)

100 mg crude A-chain **1** was used for the first step of oxidative folding. The first disulfide bond formation was carried out by oxidizing cysteines at positions A10 and A15. **1** was stirred in 25% ACN in H_2O at a 0.5 mg/mL concentration at 50 °C and DIEA was added dropwise until complete dissolution was achieved. DPDS (0.7 equivalents to the crude peptide mass) which was dissolved in methanol at a 2 mg/mL concentration was added to the solution and the resulting mixture was kept stirred at 50 °C for 30 minutes. The oxidation process was monitored by RP-HPLC analysis. After 30 minutes, a major sharp peak was observed in the analytical RP-HPLC which was characterized as oxidized product **2** (A-chain with intra-disulfide formed) (Figure 3C). Once the reaction was completed, the mixture was then purified by semi-preparative RP-HPLC and analyzed by analytical RP-HPLC and MALDI-TOF MS; *m/z* observed: 2868.01 (M+Na)+, calculated: 2867.23 (Figure 4A). A total of 26.9 mg of purified **2** was obtained (yield = 26.9%; calculated from the crude A-chain weight).

Conversion of Cys(tBu)^{A11} to Cys(SPyr)^{A11}(Scheme 2 ii.)

To form the first interchain disulfide bond, the tBu-protecting group on cysteine at position A11 was first converted to a 2-pyridylsulfenyl derivative (Scheme 2 *ii.*). 26.9 mg of purified oxidized A-chain **2** and DPDS (5 equivalents to the purified peptide) were dissolved in TFA and anisol (9:1 v/v) (65 μL/μmol of the peptide) and kept stirring in an ice bath. A solution of TFMSA/TFA (1:9 v/v, 65 μL/μmol of the peptide) was added, and the mixture was stirred for 45 minutes in an ice bath. The crude peptide was precipitated with ice-cold diethyl ether and the pellet collected by centrifugation was further washed 5 times to remove excess DPDS. The final pellet was air-dried and analyzed by RP-HPLC, which indicated that compound **3** (e.g. A-chain with Cys(SPyr)^{A11}, analytical RP-HPLC profile is shown in Figure 4B) had a loss of hydrophobicity and a reduced retention time when compared with the starting material **2** (analytical RP-HPLC profile is shown as Figure 4A). Crude compound **3** was then purified by semi-preparative RP-HPLC and analyzed by analytical RP-HPLC and MALDI-TOF MS; *m/z* observed: 2920.48 (M+Na)+, calculated 2920.27 (Figure 5A). A total of 6.5 mg of purified **3** was yielded (yield = 23.7%; calculated from the weight of purified oxidized A-chain, compound **2**).

Combination of A- and B-Chain (Scheme 2 iii.)

121 mg crude B-chain **4** was purified to obtain 44 mg purified peptide (yield = 39.4%; calculated from the weight of crude B-chain, compound **4**).

Purified **4** which was analyzed by analytical RP-HPLC and characterized by MALDI-TOF MS. *m/z* observed: 2419.089 (M+Na)+, calculated 2418.68 (Figure 5B). The first interchain disulfide bond was formed by reacting equimolar amounts of **3** and **4**. 6.5 mg of compound **3** was dissolved in 50% ACN in H_2O at a 5 mg/mL concentration and Trizma® base solution (40 mg/mL in H_2O) was added to adjust the pH of the solution of **3** to 8.5.

5.38 mg compound **4** was separately dissolved in 50% ACN in H_2O at a 2 mg/mL concentration and then dropwise added into the solution of **3**. The resulting mixture was kept stirring at ambient temperature while the progress of the reaction was monitored using analytical RP-HPLC. The reaction was complete after 20 minutes as combined product **5** was formed (Figure 5C (b)). The product was then purified by semi-preparative RP-HPLC and

analyzed by analytical RP-HPLC and MALDI-TOF MS; *m/z* observed: 5230.05 (M + Na)+, calculated 5227.79 (Figure 6A). A total of 5.5 mg of purified **5** was yielded (yield = 47.3 %; calculated from the weight of purified B-chain, compound **4**).

Iodine oxidation of the combined A- and B-chains (Scheme 2 iv.)

The Acm groups at positions A26 and B19 were removed, and a disulfide bond was formed through treatment with I_2.[29] 5.5 mg of purified intermediate **5** was dissolved in a mixture of acetic acid (3.15 mL/μmol peptide) and aqueous HCl (0.377 mL/μmol peptide) followed by the addition of 20 mM iodine/acetic acid solution (4.2 mL/μmol peptide). The mixture was stirred in the dark. After 30 minutes, the reaction was completed and the crude peptide was then precipitated by adding ice-cold diethyl ether, centrifuged, and air-dried. A small amount of the dried precipitate was analyzed using analytical RP-HPLC and showed that the final product **6** was formed as the major peak (Figure 6 B). The remaining precipitate was then resuspended in 20% ACN in H_2O with 0.1% TFA and purified by semi-preparative RP-HPLC. The final product was analyzed by RP-HPLC and MALDI-TOF MS; *m/z* observed: 5085.61 (M + Na)+, calculated 5083.62 (Figure 7 A). A total of 2.5 mg of purified **6** was yielded (yield = 46.7 %; calculated from the combination A–B product, **5**). The overall yield of Aso-RLP2 was 8.7 % calculated from the weight of purified B-chain **4**.

Regioselective Disulfide Bond Formation of Aso-RGP

The generation of synthetic Aso-RGP followed Scheme 1 under similar conditions as the regioselective disulfide bond formation of Aso-RLP2.

A-chain oxidative folding (Scheme 1 i.)

250 mg of crude A-chain **I** (Figure 2A) was utilized for the initial oxidative folding process. The formation of the first disulfide bond targeted cysteines at positions A10 and A15. Compound **I** was dissolved in a mixture of deionized water and acetonitrile (H_2O/ACN, 8:2 v/v, 2 mL/μmol). DIEA was then added dropwise to ensure the complete dissolution of the peptide. Subsequently, 0.7 equivalent of DPDS dissolved in methanol was introduced to the solution, and the mixture was stirred at room temperature. The progression of the reaction was meticulously tracked via RP-HPLC, confirming completion within 1 hour (Figure 2B). Following this oxidation reaction, the reaction mixture was directly freeze-dried, yielding 247 mg of crude product without further purification.

Conversion of Cys(tBu)^{A11} to Cys(SPyr)^{A11}(Scheme 1 ii.)

247 mg of the crude oxidized A-chain **II** was combined with 4 equivalents of DPDS in a solution of TFA and anisole (9:1 v/v). This mixture was cooled on ice before the addition of TFMSA and TFA (1:9 v/v) to initiate the reaction. The procedure was maintained at 0 °C for 45 minutes. Subsequent to the reaction, the peptide was precipitated using chilled diethyl ether, followed by at least five rounds of centrifugation to collect the crude product **III** (Figure S1A). The crude **III** was purified to obtain 20.5 mg of purified **III** (yield = 9 %, calculated from crude weight of **II**). Purified compound **III** was analyzed using analytical RP-HPLC and MALDI-TOF MS (Figure S1B and C).

Combination of A- and B-Chain (Scheme 1 iii.)

601 mg of crude material B-chain (**IV**, scheme 1, Figure S2A) was purified to obtain 307 mg of the purified compound **IV** (Figure S2B and C) (yield = 51.1 %; calculated from the weight of crude **IV**). Both purified **III** and **IV** were used as starting materials for the next-step chain-combination reaction.

To initiate the combination process, 20.5 mg of the purified **III** was dissolved in a solution of 50 % ACN in H_2O at a 5 mg/mL concentration and Trizma® base solution (40 mg/mL in H_2O) was added to adjust the pH of the solution of **III** to 8.5. Separately, 17.14 mg of the **IV** was dissolved in 50 % ACN in H_2O at a 2 mg/mL concentration and then dropwise added into the solution of **III**. The progress of the chain combination reaction was closely monitored using RP-HPLC and MALDI-TOF MS (Figure S3A and C). Following completion, the reaction mixture underwent purification through preparative RP-HPLC and was subsequently freeze-dried, yielding 18 mg of the combined A–B product (**V**, Figure S3 B) (yield = 49.7 %; calculated from the weight of purified B-chain, compound **IV**).

Iodine Oxidation of the Combined A- and B-Chains (Scheme 1 iv.)

18 mg purified **V** was dissolved in a mixture consisting of acetic acid (3.15 ml/μmol) and 60 mM HCl (0.377 ml/μmol). To this solution, 20 mM iodine in acetic acid (4.2 ml/μmol) was added, initiating the formation of the last disulfide bonds. The progress of this reaction was closely monitored using RP-HPLC. After 45 minutes, the reaction was stopped by the addition of ice-cold diethyl ether, which precipitated the peptide. This crude precipitate (Figure S4A and B) was then purified using preparative RP-HPLC and subsequently freeze-dried, yielding the 4.3 mg pure final peptide (**VI**, Aso-RGP), which features three disulfide bonds (yield = 24.5 %; calculated from the weight of purified compound **V**). The overall yield of Aso-RGP was 6.2 % calculated from purified B-chain **IV**. The final product was analyzed by analytical RP-HPLC and MALDI-TOF MS; *m/z* observed: 4776.80 (M + Na)+, calculated 4773.23 (Figure 7B).

Peptide Content Analyses

Merck Millipore Direct Detect IR spectrometer and assay-free sample cards were used to determine the peptide content. Each card has hydrophilic areas enclosed by a hydrophobic ring to keep the examined sample inside the IR beam for appropriate sample application and analysis. For measurements, all peptides were dissolved in matching solvents based on their solubility to a final concentration of 1 μg/μL, and 2 μL of sample solution was used for each measurement. The solvent served as the blank. This determines the peptide content per "spot" and is used to determine the true peptide content per weight of peptide measured, allowing true comparison of the peptide mole for mole. This analytical approach was pivotal for precisely determining the content of the purified final peptides, adjusting them to 100 % content, e.g. the accurate determination of the final yields, yielding 2.5 mg of Aso-RLP2 (purified **6**) and 4.3 mg of Aso-RGP (purified **VI**).

Circular Dichroism Spectroscopy

CD assessment of peptides was performed with a Chirascan-plus (Applied Photophysics, Leatherhead, UK). The CD spectra of the peptides were obtained at 25 °C with a 1 mm path-length cell. The peptides were dissolved in a chlorine-free phosphate buffer (PB) solution (pH 7.4). The wavelength of scanning was 190–280 nm, and the data pitch was 0.1 nm. Three accumulations were taken for

each peptide during continuous scanning at a speed of 0.5 times per point. The concentration of peptides was 40 μM. The signal was recorded as millidegree and normalized to give units of mean-residue ellipticity (MRE or q) or [θ] according to the following equation: q = mdeg/(c, l, Nres), where mdeg is the CD output in millidegrees, c is the molar peptide concentration, l is the light path length in mm and Nres is the number of amino acid residues. To ascertain the %helicity of the peptides, we employed a specific equation to calculate the $[\theta]_{222\,nm}$ for 100% helicity: $[\theta]_{222\,nm}$ for 100% helicity (**x-value**) = −40000×(1-(2.5 ÷ number of amino acids)) + (100×temperature); $[\theta]_{222\,nm}$ observed for each peptide (**y-value**); %helicity of peptide = (**x-value** ÷ **y-value**)×100.

Acknowledgements

This work was supported by National Health & Medical Research Council (NHMRC) of Australia Grants to M.A. Hossain (GNT2001178, GNT1182996); and R.A.D. Bathgate (GNT2001027) and an NHMRC Senior Research Fellowship to R.A.D. Bathgate (GNT1135837). Studies at the Florey Institute were supported by the Victorian Government's Operational Infrastructure Support Program. Open Access publishing facilitated by The University of Melbourne, as part of the Wiley - The University of Melbourne agreement via the Council of Australian University Librarians.

Conflict of Interests

The authors declare no conflict of interest.

Data Availability Statement

The data that support the findings of this study are available from the corresponding author upon reasonable request.

Keywords: Peptides · Relaxin · Insulin · RLP · RXFP1

[1] C. Schwabe, J. K. McDonald, *Science* **1977**, *197*, 914–915.
[2] G. I. Bell, R. L. Pictet, W. J. Rutter, B. Cordell, E. Tischer, H. M. Goodman, *Nature* **1980**, *284*, 26–32.
[3] E. Rinderknecht, R. E. Humbel, *J. Biol. Chem.* **1978**, *253*, 2769–2776.
[4] G. I. Bell, J. P. Merryweather, R. Sanchez-Pescador, M. M. Stempien, L. Priestley, J. Scott, L. B. Rall, *Nature* **1984**, *310*, 775–777.
[5] P. Hudson, J. Haley, M. John, M. Cronk, R. Crawford, J. Haralambidis, G. Tregear, J. Shine, H. Niall, *Nature* **1983**, *301*, 628–631.
[6] P. Hudson, M. John, R. Crawford, J. Haralambidis, D. Scanlon, J. Gorman, G. Tregear, J. Shine, H. Niall, *EMBO J.* **1984**, *3*, 2333–2339.
[7] S. Lok, D. S. Johnston, D. Conklin, C. E. Lofton-Day, R. L. Adams, A. C. Jelmberg, T. E. Whitmore, S. Schrader, M. D. Griswold, S. R. Jaspers, *Biol. Reprod.* **2000**, *62*, 1593–1599.
[8] I. M. Adham, E. Burkhardt, M. Benahmed, W. Engel, *J. Biol. Chem.* **1993**, *268*, 26668–26672.
[9] A. Koman, S. Cazaubon, P. O. Couraud, A. Ullrich, A. D. Strosberg, *J. Biol. Chem.* **1996**, *271*, 20238–20241.
[10] D. Conklin, C. E. Lofton-Day, B. A. Haldeman, A. Ching, T. E. Whitmore, S. Lok, S. Jaspers, *Genomics* **1999**, *60*, 50–56.
[11] T. N. Wilkinson, T. P. Speed, G. W. Tregear, R. A. Bathgate, *BMC Evol. Biol.* **2005**, *5*, 1–17.
[12] F. L. Hisaw, *Proc. Soc. Exp. Biol. Med.* **1926**, *23*, 661–663.
[13] a) A. Garelli, F. Heredia, A. P. Casimiro, A. Macedo, C. Nunes, M. Garcez, A. R. M. Dias, Y. A. Volonte, T. Uhlmann, E. Caparros, *Nat. Commun.* **2015**, *6*, 8732; b) S. V. Good-Avila, S. Yegorov, S. Harron, J. Bogerd, P. Glen, J. Ozon, B. C. Wilson, *BMC Evol. Biol.* **2009**, *9*, 1–19; c) S. Y. T. Hsu, *Trends Endocrinol. Metab.* **2003**, *14*, 303–309; d) R. A. Bathgate, M. Kocan, D. J. Scott, M. A. Hossain, S. V. Good, S. Yegorov, J. Bogerd, P. R. Gooley, *Pharmacol. Ther.* **2018**, *187*, 114–132.
[14] M. Mita, M. Yoshikuni, K. Ohno, Y. Shibata, B. Paul-Prasanth, S. Pitchayawasin, M. Isobe, Y. Nagahama, *Proc. Natl. Acad. Sci. USA* **2009**, *106*, 9507–9512.
[15] M. Mita, K. Yamamoto, Y. Nagahama, *Zoolog Sci* **2011**, *28*, 764–769.
[16] a) D. C. Semmens, O. Mirabeau, I. Moghul, M. R. Pancholi, Y. Wurm, M. R. Elphick, *Open biology* **2016**, *6*, 150224; b) H. D. Chieu, L. Turner, M. K. Smith, T. Wang, J. Nocillado, P. Palma, S. Suwansa-Ard, A. Elizur, S. F. Cummins, *Front. Genet.* **2019**, *10*, 77; c) J. A. Veenstra, *PeerJ* **2021**, *9*, e11799; d) M. Mita, *Biomol. Eng.* **2023**, *13*.
[17] M. S. Pratchett, C. F. Caballes, C. Cvitanovic, M. L. Raymundo, R. C. Babcock, M. C. Bonin, Y. M. Bozec, D. Burn, M. Byrne, C. Castro-Sanguino, C. C. M. Chen, S. A. Condie, Z. L. Cowan, D. J. Deaker, A. Desbiens, L. M. Devantier, P. J. Doherty, P. C. Doll, J. R. Doyle, S. A. Dworjanyn, K. E. Fabricius, M. D. E. Haywood, K. Hock, A. K. Hoggett, L. Høj, J. K. Keesing, R. A. Kenchington, B. J. Lang, S. D. Ling, S. A. Matthews, H. I. McCallum, C. Mellin, B. Mos, C. A. Motti, P. J. Mumby, R. J. W. Stump, S. Uthicke, L. Vail, K. Wolfe, S. K. Wilson, *Biol. Bull.* **2021**, *241*, 330–346.
[18] M. K. Smith, H. D. Chieu, J. Aizen, B. Mos, C. A. Motti, A. Elizur, S. F. Cummins, *Gen. Comp. Endocrinol.* **2019**, *281*, 41–48.
[19] X. Luo, R. A. Bathgate, W.-J. Zhang, Y.-L. Liu, X.-X. Shao, J. D. Wade, Z.-Y. Guo, *Amino Acids* **2010**, *39*, 1343–1352.
[20] a) M. Akhter Hossain, R. A. Bathgate, C. K. Kong, F. Shabanpoor, S. Zhang, L. M. Haugaard-Jönsson, K. J. Rosengren, G. W. Tregear, J. D. Wade, *ChemBioChem* **2008**, *9*, 1816–1822; b) A. Belgi, M. A. Hossain, F. Shabanpoor, L. Chan, S. Zhang, R. A. Bathgate, G. W. Tregear, J. D. Wade, *Biochemistry* **2011**, *50*, 8352–8361.
[21] a) M. A. Hossain, A. Belgi, F. Lin, S. Zhang, F. Shabanpoor, L. Chan, C. Belyea, H.-T. Truong, A. R. Blair, S. Andrikopoulos, *Bioconjugate Chem.* **2009**, *20*, 1390–1396; b) M. A. Hossain, R. A. Bathgate, C. K. Kong, F. Shabanpoor, S. Zhang, L. M. Haugaard-Jonsson, K. J. Rosengren, G. W. Tregear, J. D. Wade, *ChemBioChem* **2008**, *9*, 1816–1822.
[22] a) F. Lin, L. Otvos Jr, J. Kumagai, G. W. Tregear, R. A. Bathgate, J. D. Wade, *J Pept Sci* . **2004**, *10*, 257–264; b) R. A. Bathgate, F. Lin, N. F. Hanson, L. Otvos, A. Guidolin, C. Giannakis, S. Bastiras, S. L. Layfield, T. Ferraro, S. Ma, *Biochemistry* **2006**, *45*, 1043–1053.
[23] a) L. M. Haugaard-Jonsson, M. A. Hossain, N. L. Daly, R. A. Bathgate, J. D. Wade, D. J. Craik, K. J. Rosengren, *J. Biol. Chem.* **2008**, *283*, 23811–23818; b) C. S. Samuel, F. Lin, M. A. Hossain, C. Zhao, T. Ferraro, R. A. Bathgate, G. W. Tregear, J. D. Wade, *Biochemistry* **2007**, *46*, 5374–5381; c) M. A. Hossain, F. Lin, S. Zhang, T. Ferraro, R. A. Bathgate, G. W. Tregear, J. D. Wade, *Int. J. Pept. Res. Ther.* **2006**, *12*, 211–215.
[24] M. Keller, C. Sager, P. Dumy, M. Schutkowski, G. S. Fischer, M. Mutter, *J. Am. Chem. Soc.* **1998**, *120*, 2714–2720.
[25] M. Mergler, F. Dick, B. Sax, P. Weiler, T. Vorherr, *J Pept Sci.* **2003**, *9*, 36–46.
[26] J. D. Wade, F. Lin, M. A. Hossain, R. M. Dawson, *Amino Acids* **2012**, *43*, 2279–2283.
[27] O. Weil-Ktorza, N. Rege, S. Lansky, D. E. Shalev, G. Shoham, M. A. Weiss, N. Metanis, *Chem. Eur. J.* **2019**, *25*, 8513–8521.
[28] K. Hojo, M. A. Hossain, J. Tailhades, F. Shabanpoor, L. L. Wong, E. E. Ong-Palsson, H. E. Kastman, S. Ma, A. L. Gundlach, K. J. Rosengren, *J. Med. Chem.* **2016**, *59*, 7445–7456.
[29] S. Zhang, F. Lin, M. A. Hossain, F. Shabanpoor, G. W. Tregear, J. D. Wade, *Int. J. Pept. Res. Ther.* **2008**, *14*, 301–305.

Manuscript received: March 6, 2024
Accepted manuscript online: April 12, 2024
Version of record online: May 15, 2024